

The Significance of Leg Mass in Modeling Quadrupedal Running Gaits

James Schmiedeler¹, Robert Siston², and Kenneth Waldron²

¹ Department of Mechanical Engineering, University of Iowa, USA

² Department of Mechanical Engineering, Stanford University, USA

Abstract. In modeling running gaits of biological and robotic quadrupeds, leg mass is often neglected. Analysis of the system angular momentum in a biological model and a robot model indicates that including leg mass is significant in capturing the roll motion in trotting and pacing. Leg mass has a more significant effect on the pitch motion in bounding and is most critical in accurately capturing the dynamics of galloping.

1 Introduction and Background

Dynamic simulation has become an important tool in the design and control of legged robots, especially those capable of moving at high speeds with running gaits. Raibert (1986), Furusho et al. (1995), and Papadopoulos and Buehler (2000) all used simulation extensively in developing their running quadrupeds. In parallel with robot simulation, modeling has improved the understanding of dynamic locomotion in the biological world. Herr and McMahon's (2000, 2001) investigations of trotting and galloping and Wong and Orin's (1995) studies of jumping are recent examples. In simulating or modeling any type of legged locomotion, it is an ongoing challenge to capture the significant mechanics of gait while maintaining simplicity in the model. One common assumption to reduce computation is that the legs of a quadruped are massless. This paper investigates the validity of that assumption by analyzing the effect of leg mass on the dynamics of trotting, pacing, bounding, and galloping in models of a biological and a robotic quadruped.

2 Biological Model

A biological quadruped model was developed through simple and non-invasive measurements of a Labrador dog. Height, width, girth, and girdle were measured at various points of the body. The lengths and thicknesses of the leg segments, the longitudinal distance between the shoulders and hips, and the lateral distance between the shoulders and the hips were all measured. A total mass, M , of 33 kg was computed by simultaneously placing each of the feet on a calibrated scale and adding the four readings. These readings and the distances between the feet in the lateral and longitudinal directions were recorded for each of three trials, and the results were averaged. The data confirmed that the mass distribution was symmetric in the lateral direction and that the mass center was closer to the shoulders than the hips; the front legs supported 65% of the body weight.

The dog's pitch moment of inertia, I_y , was calculated by measuring her period of oscillation, T , as a compound pendulum. A denim sling with four leg holes was constructed to hold the dog in a standing posture. The sling was mounted to a rectangular aluminum frame, in turn mounted

to two bent aluminum rods. The rods were looped over a steel pipe to serve as the revolute joint for the pendulum. The dog was given a light push, and the time required for five complete oscillations was recorded. Three separate trials were completed, and the times were averaged. The corresponding pitch moment of inertia was calculated with Equation 1 to be $2.87 \text{ kg} \cdot \text{m}^2$ for a pendulum length, l , of $.86 \text{ m}$.

$$I_y = Ml^2 \left[\left(\frac{T}{2\pi} \right)^2 \left(\frac{g}{l} \right) - 1 \right]. \quad (1)$$

The dog's body structure was modeled with a combination of solid geometric primitives of uniform density. The head was modeled as a single sphere fixed to the torso which was composed of twenty elliptical cylinders. Each leg consisted of two circular cylinders connected by a revolute knee joint. Each leg was also connected to the torso with a single revolute shoulder/hip joint, so the abduction/adduction motion was neglected. Each front leg accounted for 5.1% and each hind leg for 9.1% of the total mass. The model's torso dimensions were fine-tuned such that the longitudinal position of the mass center matched that calculated from weighing the animal. The model's composite rigid body pitch moment of inertia for standing posture was calculated to be $2.80 \text{ kg} \cdot \text{m}^2$, which agrees well with the result of the pendulum experiments. Figure 1 is a profile of the model superimposed on an outline of the dog.

The leg motions of the biological model for pacing and galloping were determined by analyzing Muybridge's (1957) photographs of dogs of similar size. Line segments were drawn on each photograph to represent the positions of the thigh and shank. The angles of these line segments were then measured, and the model leg segments were set to match them for each photograph in the sequence. The pace angles came from four photographs and the gallop angles from seven photographs, in each case representing the full range of leg motions for one stride.

3 Robot Model

The robot model in Figure 2 consists of a rectangular parallelepiped body with four cylindrical legs attached by four revolute joints. This configuration allows each leg to swing in the sagittal plane, but neglects abduction/adduction motion. The legs have a fixed length, and the dimensions of the legs and body were selected to match the inertia properties of Raibert's (1986) quadruped.

To generate the leg motions for trotting, pacing, and bounding, the legs were assumed to

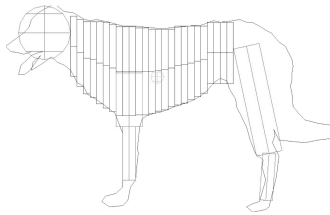


Figure 1. Outline of the Labrador's body with the geometric primitives of the model superimposed.

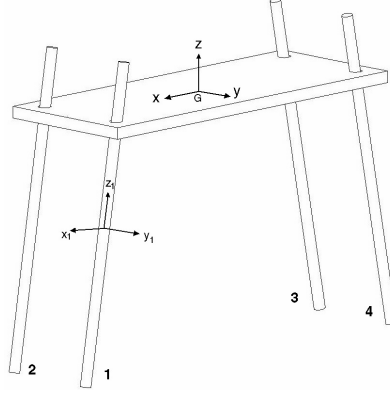


Figure 2. Quadruped robot model similar in structure to Raibert's quadruped.

move synchronously in pairs precisely out of phase with each other. The legs are employed in diagonal pairs in the trot, lateral pairs in the pace, and front/hind pairs in the bound. The range of motion of the legs was the maximum allowed by the robot design, $\pm 33^\circ$.

4 Angular Momentum

The following formulation applies to the robot model, and a qualitative extension to the biological model is presented at the end of this section. Neglecting viscous air drag, no external moments act about a quadruped's mass center during a flight phase, so the angular momentum, \mathbf{H}_G , about the mass center is conserved. Rotation of the legs relative to the body can change the body's angular velocity, $\mathbf{\Omega}$, but the angular momentum of the system remains constant and can be expressed in terms of the separate contributions of the body and the four legs,

$$\mathbf{H}_G = \mathbf{H}_{G,body} + \sum_{i=1}^4 \mathbf{H}_{G,leg_i}, \quad (2)$$

where,

$$\mathbf{H}_{G,body} = I_{G,body} \mathbf{\Omega}, \text{ and } \mathbf{H}_{G,leg_i} = I_{G,leg_i} \mathbf{\Omega} + I_{G,leg_i} \boldsymbol{\omega}_i. \quad (3)$$

$I_{G,body}$ is the inertia matrix of the body, I_{G,leg_i} is the inertia matrix of leg i , and $\boldsymbol{\omega}_i$ is the angular velocity of leg i relative to the body, all expressed relative to the coordinate system fixed in the body at the mass center. The angular momentum can be rewritten in terms of the composite rigid body inertia matrix, $I_{G,CRB}$, of the system.

$$\mathbf{H}_G = I_{G,CRB} \mathbf{\Omega} + \sum_{i=1}^4 I_{G,leg_i} \boldsymbol{\omega}_i. \quad (4)$$

The leg inertia in Equation 4 can be expanded in the form,

$$I_{G,leg_i} = R_i^T \bar{I} R_i + m(\mathbf{s}_i^T \mathbf{s}_i[1] - \mathbf{s}_i \mathbf{s}_i^T), \quad (5)$$

where \bar{I} is the inertia matrix of each leg expressed relative to its own coordinate system, R_i is the rotation matrix between the body-fixed coordinate system and the coordinate system of leg i , m is the leg mass, $\mathbf{s}_i = \{s_{ix} \ s_{iy} \ s_{iz}\}^T$ is the position vector from the body-fixed coordinate system to the coordinate system of leg i , and $[1]$ is the 3 x 3 identity matrix. Since each leg is a circular cylinder, \bar{I} is a diagonal matrix. Substituting Equation 5 into Equation 4,

$$\mathbf{H}_G = I_{G,CRB}\boldsymbol{\Omega} + \sum_{i=1}^4 R_i^T \bar{I} R_i \boldsymbol{\omega}_i + \sum_{i=1}^4 m(\mathbf{s}_i^T \mathbf{s}_i [1] - \mathbf{s}_i \mathbf{s}_i^T) \boldsymbol{\omega}_i. \quad (6)$$

Noting that $\boldsymbol{\omega}_i = \{0 \ \omega_i \ 0\}^T$ because each leg has a single degree of freedom, that all of the ω_i 's are equal in magnitude, and that two of the ω_i 's are opposite in sign to the other two because the legs move in pairs out of phase, the first summation goes to zero regardless of the joint angles. This leaves only the second summation to vary among the three gaits. Table 1 lists the parameter simplifications to be substituted into this summation for each gait.

The formulation above does not apply equally well to the biological model because the legs do not move perfectly out of phase with each other and because they have two degrees of freedom. Due to the knee flexion, the inertia matrices of these legs are not necessarily diagonal. Still, the structure and movements of the biological model bear enough similarities to those of the robot model to assume that the products of the composite rigid body moments of inertia and the corresponding body angular velocities will be the dominant terms in the angular momentum calculations. It is reasonable to investigate the changes in the composite rigid body moments of inertia with leg movement as indications of how leg mass affects the gait dynamics.

Table 1. Parameter simplifications for trotting, pacing, and bounding.

Trotting				
1	s_{1x}	s_{1y}	s_{1z}	ω_1
2	s_{2x}	$-s_{1y}$	s_{1z}	$-\omega_1$
3	$-s_{2x}$	$-s_{1y}$	s_{1z}	ω_1
4	$-s_{1x}$	s_{1y}	s_{1z}	$-\omega_1$
Pacing				
1	s_{1x}	s_{1y}	s_{1z}	ω_1
2	s_{2x}	$-s_{1y}$	s_{1z}	$-\omega_1$
3	$-s_{1x}$	$-s_{1y}$	s_{1z}	$-\omega_1$
4	$-s_{2x}$	s_{1y}	s_{1z}	ω_1
Bounding				
1	s_{1x}	s_{1y}	s_{1z}	ω_1
2	s_{1x}	$-s_{1y}$	s_{1z}	ω_1
3	$-s_{1x}$	$-s_{1y}$	s_{1z}	$-\omega_1$
4	$-s_{1x}$	s_{1y}	s_{1z}	$-\omega_1$

5 Results

Making the trotting substitutions from Table 1 in Equation 6, the angular momentum of the robot model is given by,

$$\mathbf{H}_G = I_{G,CRB}\mathbf{\Omega} + \begin{Bmatrix} -2ms_{1y}(s_{1x} + s_{2x})\omega_1 \\ 0 \\ 0 \end{Bmatrix}. \quad (7)$$

For all but the special case of $s_{1x} = -s_{2x}$ when all four legs are in the vertical position, the changes in angular momentum of moving the legs in diagonal pairs do not cancel. Since support is provided at opposite ends of the body in trotting, $\mathbf{\Omega}$ is typically negligible as the body does not rotate significantly. The second term in Equation 7 suggests, however, that the changes in angular velocity of the legs relative to the body will cause body rotation in the roll direction. Small pitch and yaw rotation would normally be expected also, except that the composite rigid body products of inertia in $I_{G,CRB}$ are uniformly zero for trotting. For all trotting motions of the robot model, the coefficient $2ms_{1y}(s_{1x} + s_{2x})$ in Equation 7 is between 30% and 40% of the composite rigid body roll moment of inertia. (A corresponding value for the biological model is non-sensical because the legs have two degrees of freedom.) This suggests that the change in the body's angular velocity would be between 30% and 40% of the legs' change in angular velocity during a flight phase. The net result is that the movement of the legs relative to the body has significant effect on the roll motion of the body in trotting.

Making the pacing substitutions from Table 1 in Equation 6, the angular momentum of the robot is simply,

$$H_G = I_{G,CRB}\mathbf{\Omega}. \quad (8)$$

The changes in angular momentum associated with the legs cancel. Since support is provided

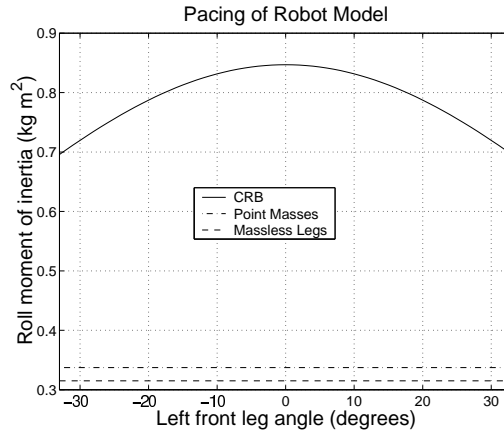


Figure 3. Roll moment of inertia for pacing of the robot model

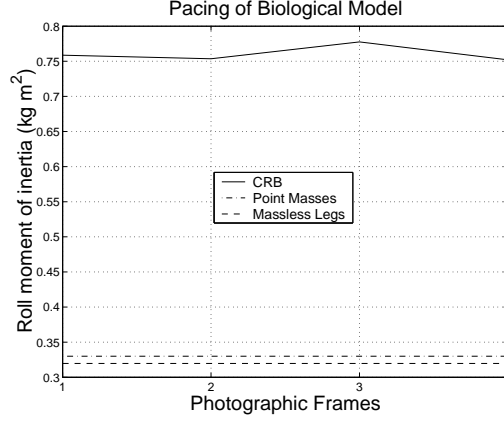


Figure 4. Roll moment of inertia for pacing of the biological model

on opposite sides of the body in pacing, Ω typically has the form $\{\Omega \ 0 \ 0\}^T$, such that the dominant rotation of the body is in the roll direction. Therefore, the dominant term in the angular momentum calculation is the product of the roll angular velocity and the composite rigid body roll moment of inertia. Figure 3 plots the roll moment of inertia for the robot model over the full range of leg motions. For comparison, the roll moment of inertia is also plotted for two simplified models: one that lumps the mass of each leg at a single point at the shoulder/hip joint and another that neglects leg mass entirely by equally distributing it within the torso. Figure 4 plots the same quantities for the biological model. Both plots clearly indicate that the simplified models underestimate the roll moments of inertia. In the case of the biological model, however, the roll moment of inertia does not change significantly with the motion of the legs. Therefore, leg mass could be neglected without loss of accuracy provided that the roll moment of inertia for the body is computed with the inclusion of the massive legs. In the robot model, the roll moment of inertia changes by as much as 18% with the motion of the legs. To accurately capture the roll motion in this case, leg mass would need to be included in the simulation.

Making the bounding substitutions from Table 1 in Equation 6, the angular momentum of the robot is again given by,

$$H_G = I_{G,CRB}\Omega. \quad (9)$$

As in pacing, the changes in angular momentum associated with the legs cancel. For bounding, however, Ω typically has the form $\{0 \ \Omega \ 0\}^T$, such that the dominant rotation of the body is in the pitch direction. Figure 5 plots the pitch moment of inertia for the robot model and the simplified models over the full range of leg motions. As with pacing, the simplified models again underestimate the critical moment of inertia. For bounding, however, the pitch moment of inertia changes even more significantly as the legs move. From a mean value when the legs are in the vertical position, it fluctuates by as much as 18% in either direction. This indicates that including leg mass in a model is even more important for accurately capturing the dynamics of the bound than it is for the pace. No data are presented for the biological model because no photos of dogs bounding were available.

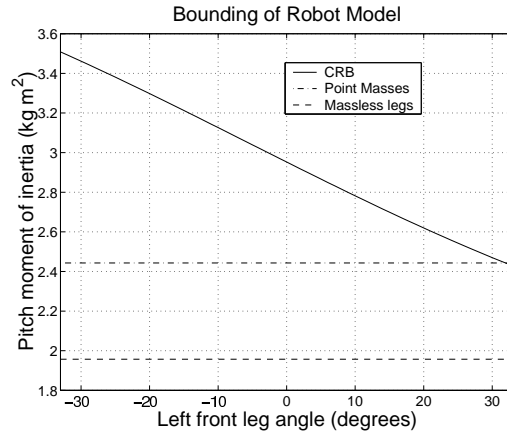


Figure 5. Pitch moment of inertia for bounding of the robot model

Figure 6 plots all three moments of inertia for galloping of the biological model. The pitching motion of the body dominates in galloping, but some roll and yaw motion are also expected because the legs operate individually. No data are presented for the robot model because no quadruped robot capable of true galloping has yet been built. No formulation for the angular momentum of a galloping model is presented either, primarily because the legs do not move synchronously in the gallop which leads to a complex expression for the angular momentum that does not provide the same insight as for the other gaits. Still, the variations in the moments of inertia give a general indication of how the motion of the legs affect the overall motion of the body.

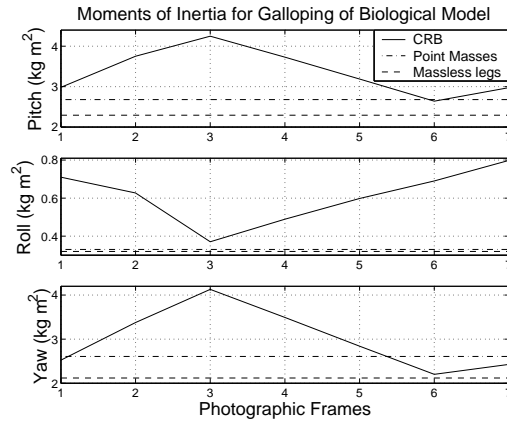


Figure 6. Moments of inertia for galloping of the biological model

As for the other gaits, the simplified models underestimate the moments of inertia in galloping. Also, comparing the plots in Figure 6 to the preceding plots for the other gaits, it is clear that all of the moments of inertia changes more significantly with the leg motions in galloping. From their mean values, the pitch moment of inertia varies positively and negatively by more than 20%, the roll moment by more than 30%, and the yaw moment by more than 25%. Therefore, including leg mass in a galloping model is even more important to capture the dynamics of the motion than it is for the other gaits. This is particularly true since the gallop is the highest speed gait for many biological quadrupeds.

6 Summary

Analyzing the changes in system angular momentum during a flight phase gives an indication of how significantly the movement of massive legs relative to the body affects the body's motion. To accurately model trotting, leg mass should be included in order to account for the roll motion of the body caused by the leg rotation. At slow speeds, though, this effect will be less significant, and the dynamics may still be accurately modeled with massless legs. For pacing, leg mass should be included at the very least in computing the roll moment of inertia of the system. That roll moment was found not to change much for the biological model, but to change significantly for the robot model. In modeling bounding, leg mass should be included because the movement of the legs has a dramatic effect on the pitch moment of inertia. Of all the gaits, leg mass is most critical in capturing the dynamics of galloping. Pitch, roll, and yaw motion are all found in galloping, and the movements of the legs have significant effect on the system moments of inertia.

The results presented in this work do not suggest that models with massless legs are without value. On the contrary, they can be very useful in explaining general phenomena and investigating many behaviors. In simulating a robotic system or developing a highly detailed account of animal locomotion, however, such models may be inadequate.

References

- Furusho, J., Akihito, S., Masamichi, S., and Eichi, K. (1995). Realization of bounce gait in a quadruped robot with articular-joint-type legs. In *Proceedings of the IEEE International Conference on Robotics and Automation*. Nagoya, Japan. 697–702.
- Herr, H., and McMahon, T. A. (2000). A trotting horse model. *International Journal of Robotics Research* 19:566–581.
- Herr, H., and McMahon, T. A. (2001). A galloping horse model. *International Journal of Robotics Research* 20:26–37.
- Muybridge, E. (1957). *Animals in Motion*. New York: Dover Publications, Inc.
- Papadopoulos, D., and Buehler, M. (2000). Stable running in a quadruped robot with compliant legs. *Proceedings of the IEEE International Conference on Robotics and Automation*. San Francisco, CA. 1146–1152.
- Raibert, M. H. (1986). *Legged Robots that Balance*. Cambridge, MA: MIT Press.
- Wong, H. C., and Orin, D. E. (1995). Control of a quadruped standing jump over irregular terrain obstacles. *Autonomous Robots* 1:111–129.